Appl Microbiol Biotechnol (2017) 101:1465–1476
DOI 10.1007/s00253-016-7899-4

GH115 α-glucuronidase and GH11 xylanase from *Paenibacillus* sp. JDR-2: potential roles in processing glucuronoxylans

Mun Su Rhee[1,2] · Neha Sawhney[1,3] · Young Sik Kim[1] · Hyun Jee Rhee[1,4] · Jason C. Hurlbert[5] · Franz J. St. John[6] · Guang Nong[1] · John D. Rice[1] · James F. Preston[1]

Received: 11 May 2016 / Revised: 13 September 2016 / Accepted: 25 September 2016 / Published online: 21 October 2016

Abstract *Paenibacillus* sp. JDR-2 (Pjdr2) has been studied as a model for development of bacterial biocatalysts for efficient processing of xylans, methylglucuronoxylan, and methylglucuronoarabinoxylan, the predominant hemicellulosic polysaccharides found in dicots and monocots, respectively. Pjdr2 produces a cell-associated GH10 endoxylanase ($Xyn10A_1$) that catalyzes depolymerization of xylans to xylobiose, xylotriose, and methylglucuronoxylotriose with methylglucuronate-linked α-1,2 to the nonreducing terminal xylose. A GH10/GH67 xylan utilization regulon includes genes encoding an extracellular cell-associated $Xyn10A_1$ endoxylanase and an intracellular GH67 α-glucuronidase active on methylglucuronoxylotriose generated by $Xyn10A_1$ but without activity on methylglucuronoxylotetraose generated by a GH11 endoxylanase. The sequenced genome of Pjdr2 contains three paralogous genes potentially encoding GH115 α-glucuronidases found in certain bacteria and fungi. One of these, Pjdr2_5977, shows enhanced expression during growth on xylans along with Pjdr2_4664 encoding a GH11 endoxylanase. Here, we show that Pjdr2_5977 encodes a GH115 α-glucuronidase, Agu115A, with maximal activity on the aldouronate methylglucuronoxylotetraose selectively generated by a GH11 endoxylanase Xyn11 encoded by Pjdr2_4664. Growth of Pjdr2 on this methylglucuronoxylotetraose supports a process for Xyn11-mediated extracellular depolymerization of methylglucuronoxylan and Agu115A-mediated intracellular deglycosylation as an alternative to the GH10/GH67 system previously defined in this bacterium. A recombinantly expressed enzyme encoded by the Pjdr2 *agu115A* gene catalyzes removal of 4-*O*-methylglucuronate residues α-1,2 linked to internal xylose residues in oligoxylosides generated by GH11 and GH30 xylanases and releases methylglucuronate from polymeric methylglucuronoxylan. The GH115 α-glucuronidase from Pjdr2 extends the discovery of this activity to members of the phylum *Firmicutes* and contributes to a novel system for bioprocessing hemicelluloses.

Keywords *Paenibacillus* sp. JDR-2 · Xylans · GH11 endoxylanase · GH115 α-glucuronidase · Biofuels and chemicals

First author credit should go to Mun Su Rhee, Neha Sawhney, and Young Sik Kim all of whom contributed equally to this work

Electronic supplementary material The online version of this article (doi:10.1007/s00253-016-7899-4) contains supplementary material, which is available to authorized users.

✉ James F. Preston
jpreston@ufl.edu

[1] Department of Microbiology and Cell Science, University of Florida, PO Box 110700, Gainesville, FL 32611, USA

[2] Xycrobe Therapeutics Inc., 3210 Merryfield Row, San Diego,, CA 92121,, USA

[3] Department of Chemistry, Vanderbilt University, Nashville, TN 37235,, USA

[4] Department of Materials Science and Engineering, Massachusetts Institute of Technology, 6-113, Cambridge, MA 02139,, USA

[5] Department of Chemistry, Physics and Geology, Winthrop University, Rock Hill, SC 29733, USA

[6] Forest Products Laboratory, United States Forest Service, The United States Department of Agriculture, Madison, Madison,, WI 53726, USA

Introduction

Lignocellulosic biomass resources have become viable alternatives to petroleum-based resources for production of fuels and chemicals. Derived from various sources, including timber, energy crops, and agricultural and forest product residues,

lignocellulosics contain 41–51 % cellulose and 23–38 % hemicellulose (Ragauskas et al. 2006; Saha 2003). For conversion of these resources to biofuels and chemicals, pretreatments of lignocellulosic biomass at high temperatures with strong acids have been applied to provide cellulose that is more accessible to cellulases and at the same time solubilize xylans and release pentoses from the hemicellulose (Mosier et al. 2005). Efforts to develop microbial biocatalysts for production of biofuels that secrete cellulases show promise for mitigating the requirement for their addition and associated cost (Chundawat et al. 2011; Lynd et al. 1999; Olson et al. 2012).

Other pretreatment strategies, including alkaline and ammonia fiber expansion (AFEX), offer some advantages over acid pretreatment with respect to engineering design costs and allow solubilization of xylans with diminished generation of products toxic to biocatalysts that occurs with acid hydrolysis. Hemicellulases are then required to convert the hemicellulose fractions to fermentable pentoses. Acidic xylans with methylglucuronate substitutions represent the predominant source of fermentable pentoses in the hemicellulose fractions of lignocellulosic biomass and are solubilized and deesterified by alkaline pretreatment. These include methylglucuronoxylans ($MeGX_n$) extracted from dicots including hardwoods, as well as gymnosperms including softwoods, and methylglucuronoarabinoxylans ($MeGAX_n$) from monocots, including energy crops and agricultural residues.

Further processing of alkaline extracts requires the addition of hemicellulases, including endoxylanases, arabinofuranosidases, β-xylosidases, and α-glucuronidases, to optimally convert soluble xylans to fermentable pentoses, providing additional costs to the bioconversion process (Preston et al. 2003; Dodd and Cann 2009; Menon and Rao 2012). As in the case for biocatalysts secreting cellulases, there is an interest in developing microbial biocatalysts for the secretion of enzymes for the digestion of $MeGX_n$ and $MeGAX_n$ solubilized by alkaline pretreatment.

Some xylanolytic bacteria secrete GH10 xylanases that generate xylotriose, xylobiose, and the aldouronate 4-*O*-methylglucuronosyl-α-1,2-xylosyl-β-1,4-xylosyl-β-1,4-xylose ($MeGX_3$ or UXX) and also have genes encoding intracellular GH67 α-glucuronidases for removing methylglucuronate (MeG), allowing conversion of xylotriose derived from $MeGX_3$ to fermentable xylose (Shulami et al. 1999; Chow et al. 2007; Nong et al. 2009; Weber et al. 2010; Shaw et al. 2008; Talluri et al. 2013; Han et al. 2012). This GH10/GH67 system for complete processing of $MeGX_n$ has been studied in some detail in species of *Geobacillus* and *Paenibacillus* (Shulami et al. 1999; St. John et al. 2006a; Chow et al. 2007; Nong et al. 2009). The efficient utilization of $MeGX_n$ by *Paenibacillus* sp. JDR2 (Pjdr2) has been ascribed to a xylan utilization regulon that encodes a secreted cell-associated GH10 endoxylanase, transcriptional regulators, ABC transporters, and intracellular glycoside hydrolases, including a GH67 α-glucuronidase. Collectively, these enzymes contribute to the efficient depolymerization of $MeGX_n$ coupled to the assimilation and metabolism of products of extracellular depolymerization (St. John et al. 2006a; Nong et al. 2009). The sequenced genome of Pjdr2 has allowed a transcriptomic analysis following growth on $MeGX_n$ or $MeGAX_n$ that supports the role of the GH10/GH67 xylan utilization regulon for the efficient utilization of hemicellulosic polysaccharides (Chow et al. 2012; Sawhney et al. 2015). The transcriptome study also showed the enhanced expression of genes encoding a GH11 endoxylanase and a putative GH115 α-glucuronidase upon growth on $MeGX_n$ or $MeGAX_n$.

In the study described here, a recombinant GH115 α-glucuronidase from the firmicute Pjdr2 has been evaluated for comparison with enzymes encoded by orthologous genes in the bacteria, *Bacteroides ovatus* (Rogowski et al. 2014) and *Streptomyces pristinaespiralis* (Fujimoto et al. 2011), and the fungi, *Schizophyllum commune* (Tenkanen and Siika-aho 2000; Kolenová et al. 2010; Chong et al. 2011) and *Pichia stipitis* (Kolenová et al. 2010). As in the case of these recent studies, the GH115 α-glucuronidase Agu115A from Pjdr2 shows similar substrate specificities that distinguish these enzymes from the GH67 α-glucuronidases which have been implicated in the bioconversion of methyglucuronoxylans. The ability of Pjdr2 to utilize the products of a GH11 endoxylanase for growth supports a process catalyzed by the secreted GH11 endoxylanase and the intracellular GH115 α-glucuronidase for the utilization of xylans comprising hemicellulosic biomass.

Materials and methods

Growth and maintenance of *Paenibacillus* sp. JDR-2 cultures

Pjdr2 cultures were routinely maintained on Zucker-Hankin defined medium (Zucker and Hankin 1970) supplemented with sweetgum $MeGX_n$. Stocks were stored at −80 °C, resuscitated, and cultured at 30 °C with aeration as previously described (St. John et al. 2006a). Specific conditions with different substrates are noted for individual experiments. A Pjdr2 culture has been deposited with the Bacillus Genetic Stock Center at Ohio State University, Columbus Ohio, as BGSC 35A1.

Preparation of substrates

Substrates for enzyme and growth studies were prepared from sweetgum $MeGX_n$ (Hurlbert and Preston 2001) and sorghum $MeGAX_n$ (Sawhney and Preston 2014). Oligoxylosides containing α-1,2-linked methylglucuronates, referred to as aldouronates, include methylglucurono-α-1,2-xylose (U)

prepared from acid hydrolysates; methylglucuronoxylotriose (UXX) generated by the digestion of $MeGX_n$ with a GH10 endoxylanase from Pjdr2 in which the methylglucuronate product is α-1, 2-linked to the nonreducing terminus (Nong et al. 2009); XUX (methylglucuronoxylotriose with the methylglucuronate linked to xylose penultimate to both reducing terminal and nonreducing terminal xyloses) prepared from cultures of *Bacillus subtilis* 168 secreting both GH11 and GH30 xylanases; XUXX prepared from cultures of *B. subtilis* MR42, secreting only a GH11 xylanase; and a mixture of acidic xylooligosaccharides, XX_nUX, with n ranging from 1 to 15 with an average of 7.2, prepared from cultures of *B. subtilis* MR44 secreting only the GH30 xylanase (Rhee et al. 2014). Abbreviations of structures that identify the xylose residues modified with α-1,2-linked methylglucuronate (U) residues are those previously used for the studies of enzymes that act on aldouronates formed following depolymerization of methylglucuronoxylans (Rogowski et al. 2014). Methylglucuronate was prepared by the digestion of UXX with recombinant Agu67 derived from Pjdr2 (Nong et al. 2009).

Preparation and characterization of recombinant enzymes

The GH11 xylanase, BsXyn11A, from *B. subtilis* 168 was prepared as a recombinant enzyme as previously described (Rhee et al. 2014). Recombinant GH67 α-glucuronidase, Agu67 from Pjdr2, was prepared as previously described (Nong et al. 2009). The recombinant GH115 α-glucuronidase, Agu115A from Pjdr2, encoded by the gene Pjdr2_5977, was cloned using primers 5′-GCA TCG GTC GAC ATG CTG AAC GAC AAC TAT ATC GC-3′ and 5′-TAT CGC TCA CCG TTC TCC AA-3′ to amplify the complete gene which was then expressed in *Escherichia coli* Rosetta DE3 (Novagen, La Jolla, CA) for production of the enzyme. Pjdr2 Xyn11 endoxylanase was produced with the same approach, but using primers 5′-GAC TCG CAT ATG GCA ACA GAC TAC TGG CAG AAC-3′ and 5′-CGT CTG GGA TCC GAG CAA GCG CTA ACC AAG AT-3′ to amplify the Pjdr2_4664 gene. Methods for gene amplification, gene sequencing, over-expression, and purification of recombinant enzymes were the same as previously described (Rhee et al. 2014). All recombinant gene products were analyzed by SDS-PAGE to establish purity and mass (Fig. S1 in the Supplementary Material). Samples of crude extracts or purified proteins were denatured in SDS buffer with β-mercaptoethanol, boiled for 10 min, delivered to 4–15 % gradient polyacrylamide gels (Bio-Rad Labotatores, Inc., Los Angeles, CA) equilibrated with 0.1 % SDS buffer, subjected to electrophoresis, and stained with 0.1 % Coomassie Blue following protocols previously described (Laemmli 1970; www.bio-rad.com).

Enzyme assays and product analysis

Endoxylanase activity was determined by estimating the increase of reducing sugar termini (Nelson 1944) as previously described (St. John et al. 2006b). The α-glucuronidase activity was determined by measuring the release of substrate for uronate dehydrogenase-catalyzed formation of glucarate coupled to NAD reduction (Yoon et al. 2009). Uronate dehydrogenase (UDH) from *Pseudomonas syringae* DC3000 was prepared as a recombinant enzyme from the *E. coli* Rosetta DE3 strain used above, with primers 5′-GACT CGCATATGGCATCGGCTCATACCACTCAAACTCC-3′ and 5′-GGCTTA GGATCCGCTTGTTCACGCAC GCTCCA-3′ to amplify *udh* (PSPTO_1053), followed by induction and over-expression methods described above. The UDH-catalyzed oxidation of glucuronate (or 4-*O*-methylglucuronate) to glucarate (or methylglucarate) is coupled to reduction of NAD to NADH which can be quantified by measurement of absorbance at 340 nm (A340). One unit catalyzes the formation of 1 μmol NADH, equivalent to a 1-μmol oxidation of aldehyde C1 of methylglucuronate released by α-glucuronidase per minute under the assay conditions. This thermodynamically unfavorable reaction requires the determination of A340 over the early portion of the reaction as equilibrium is reached with NADH at 0.1 mM, as well as 3 mM glucuronate and 1 mM NAD (data not shown). Identification of products was carried out using thin layer chromatography (TLC) and high-performance liquid chromatography (HPLC) as previously described (Nong et al. 2009; Su et al. 2011).

Growth and utilization of aldouronates by Pjdr2

The initial inocula for Pjdr2 cultures were prepared as described previously (Sawhney and Preston 2014). For growth studies, Pjdr2 was cultured in 16 × 100-mm culture tubes at 30 °C with gyrotary agitation at 220 rpm containing 3.5 mL Zucker-Hankin (ZH) minerals (pH 7.4) (Zucker and Hankin 1970) medium supplemented with 0.05 % yeast extract and 0.1 % aldouronates. Samples were removed at timed intervals to determine optical density (OD) at 600 nm, total cell protein, and total carbohydrate remaining in the culture supernatants as previously described (Nong et al. 2009).

Phylogenetic relationships of GH115 enzymes

The Clustal Omega program (Sievers et al. 2011) was used for alignment of amino acid sequences, and the phylogenetic tree was calculated from the multiple sequence alignment using the Neighbor-Joining method with the BLOSUM62 substitution matrix in Jalview (Waterhouse et al. 2009). Sequences were obtained from NCBI database for *B. ovatus* (BoAgu115A, BACOVA_03449), *S. pristinaespiralis*

(SpAgu115A, SSDG_01527T0), *Aspergillus oryzae* (AoAgu115, BAE56806), *Bacteroides thetaiotaomicron* (BtAgu115A, PDB ID: 5BY3, BT_2958), *S. commune* (ScAgu115, ADV52250), *Neurospora crassa* (NcAgu115A, NCU06143), *P. stipitis* (PsAgu115, PICST_61283), and Pjdr2 Agu115A. The *A. oryzae* and *N. crassa* sequences are putative GH115 enzymes orthologous to the characterized GH115 α-glucuronidase sequences from the other organisms.

Structural modeling of α-glucuronidases

Homology models of the Pjdr2 Agu115A were made using iTasser (Yang et al. 2015) and Phyre2 (Kelley et al. 2015). The lowest energy models generated were analyzed with Molprobity (Chen et al. 2010). Structural superpositions of the best model with the known X-ray crystallographic structures of the α-glucuronidases from *B. ovatus* (PDB ID: 4C90) and *B. thetaiotaomicron* (PDB ID: 5BY3) were performed in Chimera (Pettersen et al. 2004).

TLC analysis of xylan digestion products generated by recombinant Pjdr2 enzymes

Recombinant forms of Pjdr2 enzymes were used in these experiments. Reactions containing 0.2 % sweetgum $MeGX_n$ in the presence of 0.5 unit of each enzyme in 50 mM sodium acetate, pH 6.0, were incubated at 30 °C for 24 h. Reaction products (200 nmol xylose equivalents/sample) were analyzed by TLC with samples spotted on silica gel 60 0.25-mm plates (Merck, Darmstadt, Germany, EMD Millipore, USA). Development was made using chloroform-acetic acid-water in the ratio 6:7:1 (*v*:*v*:*v*), and products were detected as previously described (Nong et al. 2009). In some experiments, the reaction mixtures were filtered to separate the lower molecular weight oligosaccharides from the undigested polysaccharide and the enzymes. The filtration was carried out using the Amicon Centriprep 3000 MWCO filter device (EMD Millipore, Darmstadt, Germany) centrifuged at 3000 rpm (Sorvall RC-3 swinging bucket rotor). In some experiments, the first development in chloroform-acetic acid-water, 6:7:1 (*v*:*v*:*v*), was followed by a second development in ethyl acetate-acetic acid-water, 2:1:1 (*v*:*v*:*v*) (Chow et al. 2016), to resolve the xylose and MeG components.

Catabolite regulation of expression of *xyn11* and *agu115*

Gene expression levels are reported as RPKM (reads per kilobase per million reads sequenced) values obtained from triplicate growth studies and RNA-seq total transcriptome analysis (Sawhney et al. 2015). Results were combined and averaged and then normalized over the entire data set of several different growth conditions. ANOVA analysis of the total data set was performed and significant values are judged as having *p* values less than 0.01. Data sets for the results are available in the JGI Genome Portal repository, Project ID 1023680, at http://genome.jgi.doe.gov/pages/projectStatus.jsf?db=Paespnscriptome. The 14-base canonical sequence representing catabolite responsive element (*cre*) sites that were identified for glucose catabolite repression in *Geobacillus stearothermophilus* upstream of genes responsive to such transcriptional repression (Cho and Choi 1999) were used for searching for *cre* sites in the genes encoding the GH11/GH115 system in Pjdr2.

Results

Production and properties of Pjdr2 Agu115A

Gene Pjdr2_5977 (Sawhney et al. 2015) has been designated as *agu115A* encoding a protein with a sequence homologous to characterized GH115 α-glucuronidases from selected bacteria and fungi (Ryabova et al. 2009; Chong et al. 2011; Fujimoto et al. 2011; Rogowski et al. 2014). The purification of recombinant Pjdr2 Agu115A results in a single protein band by SDS-PAGE with a molecular mass of approximately 100 kDa (Fig. S1 in the Supplementary Material) and spectral properties, including an extinction coefficient 224,740 M^{-1} cm^{-1} at 280 nm measured in water, predicted by the ExPasy ProtParam program (http://web.expasy.org/protparam/) for the cloned sequence that includes six histidine residues on the amino terminus. Two other genes, Pjdr2_1125 and Pjdr2_5528, encoding proteins with significant homology to GH115 enzymes, were also cloned for production of proteins. While crude extracts of cultures of these clones produced proteins of the expected size for their respective encoding genes, no activities which released MeG from $MeGX_n$ were detected by TLC as seen for *E. coli* cultures expressing the recombinant Pjdr2 agu115A gene (Pjdr2_5977, data not shown), and these were not studied further.

Enzyme properties and substrate preferences

Enzyme activities were compared on different substrates using the kinetic assay for α-glucuronidase coupled to UDH-mediated oxidation of glucuronate to glucarate and reduction of NAD to NADH (Yoon et al. 2009). The kinetic curves for these assays shown in Fig. 1 allowed the assignment of rates of reaction under different conditions and determination of specific activities with different substrates. Activities were proportional to the amount of enzyme added for both XUXX and $MeGX_n$, and similar relationships were found for other oligosaccharides and $MeGAX_n$ (data not shown), providing zero-order kinetics with rates approximating V_{max} for making comparisons of specific enzyme activities.

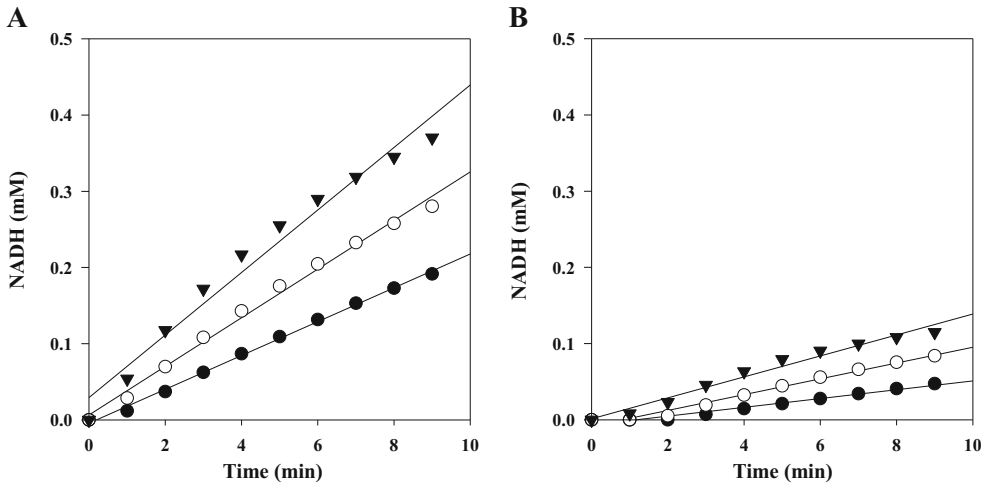

Fig. 1 Kinetic comparison of recombinant Pjdr2 GH115A activities with substrates **a** XUXX and **b** $MeGX_n$. To 0.10-ml reaction mixtures containing 100 μg substrate, increasing concentrations of the recombinant Agu115A enzyme were added followed by incubation at 30 °C. At indicated times, samples were assayed for methylglucuronate with uronate dehydrogenase-catalyzed oxidation to methylglucurate coupled to NAD reduction to NADH as described in the "Materials and methods" section. Reactions contained 10 μg (*filled circles*), 20 μg (*open circles*), or 40 μg (*filled inverted triangles*) of enzyme

The data presented in Table 1 show greatest activity for Pjdr2 Agu115A with XUXX as substrate and also significant activities with polymeric $MeGX_n$ derived from wood (sweetgum) as well as $MeGAX_n$ derived from bagasse (sweet sorghum). Pjdr2 Agu115A shows more than 16.6 times the activity on XUXX, the aldouronate limit product of a Xyn11 xylanase, than on UXX, the aldouronate limit product of a Xyn10 xylanase. Relative substrate preference follows the order of XUXX > polymeric $MeGX_n$ > XX_nUX (product of Xyn30 digestion) > XUX (product of Xyn11 and Xyn30) > polymeric $MeGAX_n$ >> UXX (product of Xyn10 digestion) > U (methylglucuronoxylose generated by acid hydrolysis). A comparison of the activities of Pjdr2 Agu115A with homologous enzymes secreted by the fungi, *P. stipitis* (Ps Agu115) and *S. commune* (Sc Agu115), is also noted in Table 1. These data, obtained from published studies (Kolenová et al. 2010), shows Sc Agu115 with a slight preference for XUXX generated by Xyn11 and XUX generated by the combined action of Xyn11 and Xyn30 compared to UXX generated by Xyn10. Ps Agu115 previously showed a slightly greater preference for UXX compared to XUX and XUXX.

Table 1 Comparison of activities of Agu115A from Pjdr2 and published activities of GH115 enzymes from other species with respect to substrate preference

Substrate	Specific activity [μmol min^{-1} mg^{-1}]		
	Pjdr2[a]	*S. commune*[b]	*P. stipitis*[b]
XUXX	16.3 (± 0.30)	7.7 (± 0.3)	2.6 (± 0.1)
$MeGX_n$	5.88 (± 0.38)	ND	ND
XX_nUX	2.88 (± 0.08)	ND	ND
XUX	1.68 (± 0.03)	7.3 (± 0.2)	4.5 (± 0.3)
$MeGAX_n$	1.50 (± 0.03)	ND	ND
UXX	0.98 (± 0.08)	5.0 (± 0.2)	4.7 (± 0.2)
U	0.56 (± 0.06)	1.2 (± 0.1)	1.2 (± 0.1)

ND not determined

[a] Recombinant Pjdr2 Agu115A activities determined as formation of NADH with the coupled uronate dehydrogenase assay

[b] Native GH115 activities from *Schizophyllum commune* and *Pichia stipitis* determined with a colorimetric assay for the release of methylglucuronate were abstracted from Fig. 2 in Kolenová et al. (2010)

Pjdr2 Agu67 shows no detectable activity toward $MeGX_n$ as there is no change in the intensity in the spotted reaction mixtures incubated for 24 h with and without the addition of Agu67 (Fig. 2). Treatment of $MeGX_n$ with Agu115A results in partial yet significant release of a product with a mobility corresponding to MeG. With UXX, hydrolysis with Agu67 produced equivalent quantities of MeG and X_3. Pjdr2 Agu115A released a small amount of MeG and X_3, from UXX, estimated at less than 5 % of the MeG released from polymeric $MeGX_n$. With XUXX as substrate, Agu67 shows no release of MeG, whereas Pjdr2 Agu115A catalyzes the quantitative release of MeG and X_4 from the XUXX substrate.

Amino acid sequence alignment, phylogenetic comparisons, and homology model analysis

The amino acid sequence of Pjdr2115A was aligned with sequences of other characterized α-glucuronidases in the GH115 family acting on glucuronoxylans, including two from fungi, *P. stipitis* (PICST_61283) (Kolenová et al. 2010) and *S. commune* (ADV52250) (Chong et al. 2011), and two from bacteria, *B. ovatus* (BACOVA_03449) (Rogowski et al. 2014)

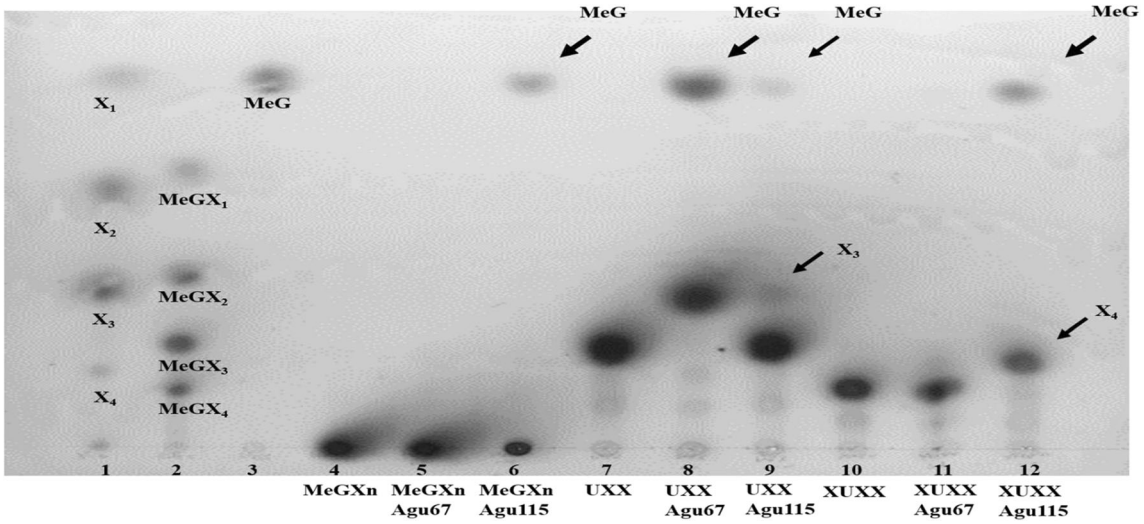

Fig. 2 Comparison of Pjdr2 Agu67 and Pjdr2 Agu115A for substrate specificity and products formed. Substrates (0.5 % $MeGX_n$, 0.5 % UXX, or 0.5 % XUXX) were incubated for 24 h with either 0.5 units of Pjdr2 Agu67 or 0.5 units of Pjdr2 Agu115A, and reactions were subjected to TLC analysis as described in the "Materials and methods" section. *Lane 1*, xylooligosaccharide standards 10 nmol each of X_1, X_2, X_3, and X_4; *lane 2*, aldouronate standards 10 nmol each of U ($MeGX_1$), UX ($MeGX_2$), UXX ($MeGX_3$), and XUXX ($MeGX_4$); *lane 3*, 10 nmol methylglucuronate (MeG) standard. *Lanes 4–6*, $MeGX_n$ substrate; *lanes 7–9*, UXX substrate, *lanes 10–12*, XUXX substrate, comparing conditions without enzyme, with Agu67 or with Agu115. Samples (0.01 ml) of reactions containing 330 nmol xylose equivalents were spotted, plates were subjected to development in chloroform/acetic acid/water solvent, and products were detected as described in the "Materials and methods" section

and *S. pristinaespiralis* (SSDG_0152T0). In addition to the amino acid sequences for these characterized enzymes, orthologous sequences for putative α-glucuronidases for *N. crassa* (NCU06143) and *A. oryzae* (BAE56806) were included. Sequence and phylogenetic comparisons of these candidates identified Pjdr2 Agu115A in a group with amino acid sequences similar to the GH115 from *B. ovatus*, *Bo*Agu115A, and another group that included GH115 α-glucuronidases from fungi (Figs. S2 and S3 in the Supplementary Material), with the sequences for the fungal enzymes providing a cluster that suggests their evolution occurring from the bacterial sequences. An orthologous Agu115 that removes MeG from acacia gum but not from glucuronoxylans is encoded by a gene from *B. thetaiotaomicron* (Aalbers et al. 2015). A structural definition of this enzyme has identified a basis for this specificity and expanded the GH115 family to include a subfamily with a role other than the processing of xylans.

The X-ray crystallographic structures of both the *B. ovatus* and *B. thetaiotaomicron* GH115 proteins were used as templates for construction of the homology model of Pjdr2 Agu115A. This model predicts the same four-domain structure as the Agu115A from *B. ovatus* (Rogowski et al. 2014) (Fig. S4 in the Supplementary Material). However, the amino acid sequence spanning Ser648 to Met769, which has no homology to known structures in the NCBI PDB database, was not properly represented by the modeling programs and was therefore removed. Based upon the structural superposition of the Pjdr2 Agu115A homology model with the crystal structures of the Agu115A proteins from *B. ovatus* and *B. thetaiotaomicron* (Fig. 3), the likely catalytic residues of Pjdr2 Agu115A are Asp303 (nucleophile) and Glu350 (proton donor). An arginine (Arg299 in Pjdr2) is conserved in all the Agu115 enzymes considered and is known to play a role in substrate binding by interacting with the C-6 carboxylate of MeG. The xylose-binding cleft bounded by Trp249 and Val426 in the *B. ovatus* Agu115A is predicted to be lined by Trp272 and Met401 in the Pjdr2 Agu115A model. The substitution of methionine in the Pjdr2 Agu115A for the valine found in the *B. ovatus* protein is not expected to significantly affect substrate binding given the conserved hydrophobic nature of the substitution.

Properties of Pjdr2 Xyn11

Recombinant Pjdr2 Xyn11 endoxylanase from Fig. S1 in the Supplementary Material had specific activities of 48.1 units/mg (+/− 0.99) with sweetgum $MeGX_n$ as substrate and 12.9 units/mg (+/− 0.28) with sorghum $MeGAX_n$ as substrate as determined in duplicate with the release of reducing termini. One unit equals the release of 1 μmol equivalent of xylose per minute under the conditions described in the "Materials and methods" section. The specific activity with $MeGX_n$ is comparable to 37 units/mg with Xyn11A from *B. subtilis* (Rhee et al. 2014). *B. subtilis* Xyn11A has been shown to generate XUXX as a limit product along with X_3 and X_2 (Rhee et al. 2014). Under similar conditions, Pjdr2 Xyn11 generates significant amounts of XUX along with XUXX, X_3, and X_2 (Fig. 4). It is clear that Pjdr2 Xyn11 generates

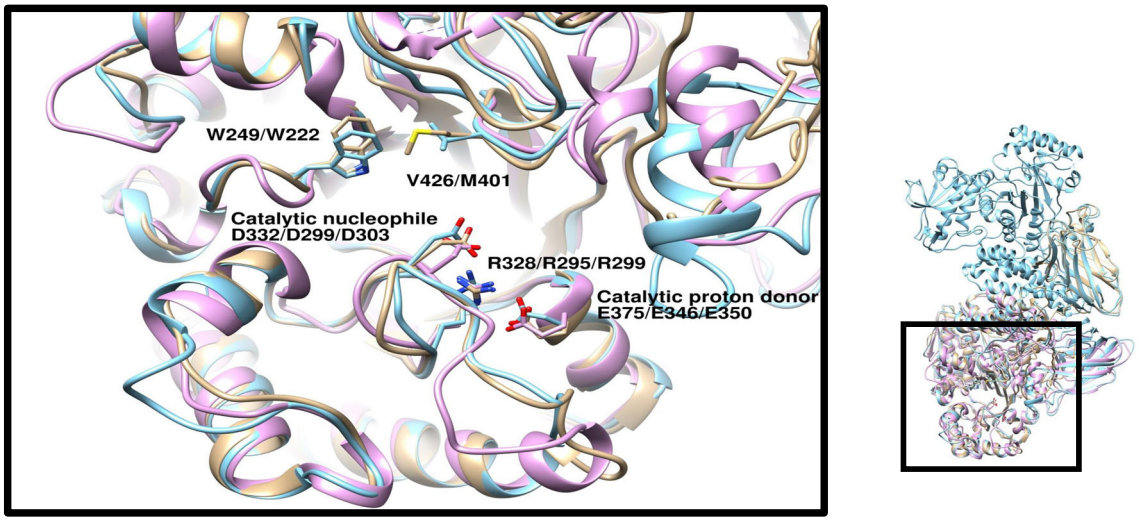

Fig. 3 Structural superposition of the homology models with the X-ray crystallographic structures of the Agu115A proteins from *B. ovatus* and *B. thetaiotaomicron*. The active sites of the superposed Agu115 proteins from *B. ovatus* (*blue*), *B. thetaiotaomicron* (*purple*), and Pjdr2 (*tan*) are seen. Catalytic amino acids are numbered in the order *B.ovatus*/*B.thetaiotaomicron*/PJDR2. Residues that are predicted to interact with xylose in the *B. ovatus* (W249 and V426) and Pjdr2 Agu115A (W222 and M401) proteins are also shown. (Color figure online)

aldouronate products that are completely processed to X_2, X_3, and MeG by Pjdr2 Agu115.

Processing and utilization of $MeGX_n$ by GH10/GH67 and GH11/GH115 systems in Pjdr2

To compare the GH10/GH67 and GH11/GH115 xylan utilization systems in Pjdr2, the xylan digestion products generated by these enzymes were examined (Fig. 4). With TLC plate development in two different solvents, the MeG standard shows mobility slightly less than xylose and is not retained on a 3000 MWCO filter. The polymeric $MeGX_n$ did not move from the origin and was completely removed by filtration. Pjdr2 $Xyn10A_1$ generates $MeGX_3$ (UXX), X_1, and X_2 as the predominant limit products, and the inclusion of Pjdr2 Agu67 along with $Xyn10A_1$ shows the complete conversion of UXX to MeG, X_1, and X_2. Pjdr2 Xyn11 generates both $MeGX_4$ (XUXX) and $MeGX_3$ (XUX) along with X_1, X_2, and X_3.

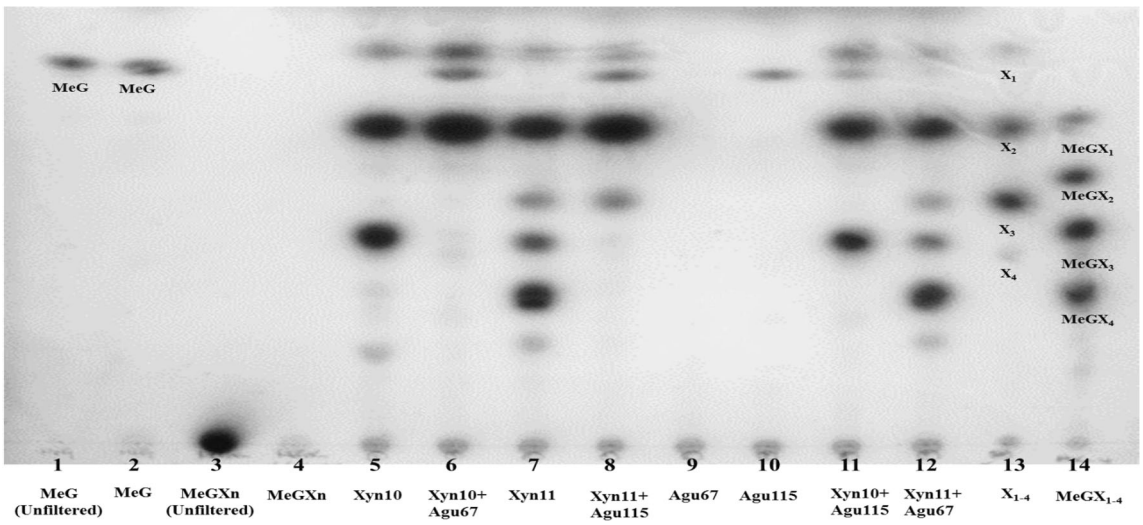

Fig. 4 Processing of $MeGX_n$ by GH10/GH67 and GH11/GH115 systems in Pjdr2. Products generated by the action of recombinant Pjdr2 Xyn11 and/or Agu115A and/or Agu67 or $Xyn10A_1$ and/or Agu115A and/or Agu67 with sweetgum $MeGX_n$ as substrate. The enzymes (0.5 units of each) were incubated in 100-μl reaction mixtures containing 0.2 % sweetgum $MeGX_n$ in 50 mM sodium acetate buffer, pH 6.5, at 30 °C for 16 h. Except for *lanes 1* and *3*, samples were filtered and resolved by TLC with plate development in chloroform/acetic acid/water (6:7:1) followed by a second development in ethyl acetate/acetic acid/water (2:1:1) as described in the "Materials and methods" section. *Lane 1*, MeG unfiltered; *lane 2*, MeG prefiltered; *lane 3*, $MeGX_n$ unfiltered; *lane 4*, $MeGX_n$ prefiltered; *lane 5*, $Xyn10A_1$; *lane 6*, $Xyn10A_1$/Agu67; *lane 7*, Xyn11; *lane 8*, Xyn11/Agu115; *lane 9*, Agu67; *lane 10*, Agu115; *lane 11*, $Xyn10A_1$/Agu115; *lane 12*, Xyn11/Agu67; *lane 13*, xylose (X_1) 10 nmol, xylobiose (X_2) 10 nmol, xylotriose (X_3) 20 nmol, xylotetraose (X_4) 10 nmol; *lane 14*, $MeGX_1$, $MeGX_2$, $MeGX_3$, and $MeGX_4$ aldouronates, 10 nmol each

The inclusion of Pjdr2 Agu115A along with Xyn11 shows complete conversion of XUXX and XUX to MeG, X_1, X_2, and X_3 (Fig. 4). The incubation of Agu115A with Xyn11 also shows release of MeG in quantities observed for the release of MeG with XUXX as a preferred substrate (Fig. 2). Incubation of $MeGX_n$ or XUXX with Agu67 shows no release of MeG. Incubation of $MeGX_n$ with Agu115A shows significant release of MeG in quantities comparable to that seen with combination of Xyn11 and Agu115A, indicating that Agu115A efficiently removes MeG from polymeric $MeGX_n$. Xyn11 with Agu67 did not release detectable MeG as expected from previous studies on the specificity of GH67 α-glucuronidases for UXX or a substrate in which 4-*O*-methylglucuronate is α-1,3-linked to the reducing terminal xylose in β-1,4-linked xylooligosaccharides (Nong et al. 2009). Agu115A did release some MeG from UXX, the product generated by $Xyn10A_1$ (Figs. 2 and 4), indicating some activity that was also seen in Table 1.

To understand the role the GH115 and the GH67 α-glucuronidases might contribute to the metabolic potential of Pjdr2, cultures were grown on the products generated from $MeGX_n$ by each enzyme and compared with growth on and utilization of $MeGX_n$ and methylglucuronoxylose (U) prepared from dilute acid hydrolysates of $MeGX_n$ (Fig. 5). Growth measured as total cell protein (Fig. 5a) was most rapid with $MeGX_n$ followed by UXX followed and XUX followed by U followed by XUXX. Rates and extent of substrate utilization were proportional to rates and growth yields (Fig. 5b).

Carbon catabolite repression of Xyn11/Agu115 and Xyn10/Agu67 systems in Pjdr2

Transcriptomic studies following growth of Pjdr2 on different substrates (Sawhney et al. 2015) showed coordinate expression of *agu115A* and *xyn11* and expression of a GH10/GH67 xylan utilization regulon. Both *agu115A* and *xyn11* showed increased expression levels on sweetgum- and sorghum-derived xylans. The RPKM values of *agu115A* were 268.8 and 169.4 on sweetgum- and sorghum-derived xylans, respectively, compared to yeast extract (YE) cultures without carbohydrate supplementation serving as controls, with only 5.2 as the RPKM value. The RPKM values of *xyn11* were 14.6 and 104.8 on sweetgum- and sorghum-derived xylans, respectively, compared to YE controls with 2.1 as the RPKM value. However, the expression of both these genes was lower during Pjdr2 growth on glucose (Fig. 6). *agu115A* and *xyn11* showed 4.3 and 0.4 as RPKM values, respectively, on glucose as substrate (Sawhney et al. 2015, 2016). The candidate *cre* sequences were identified by screening the upstream regions of the *xyn11* and *agu115A* genes in Pjdr2 and are listed in Table 2. These data support a system in which the expression of *agu115A* and *xyn11* genes in Pjdr2 is subject to catabolite repression by glucose.

Discussion

Of the three genes, Pjdr_1125, 5528, and 5977, with some degree of homology to genes encoding previously characterized GH115 α-glucuronidases, only Pjdr2_5977 provided a recombinant product that showed activity on $MeGX_n$. In contrast to Pjdr2 Agu115A, Sc Agu115 from *S. commune* and Ps Agu115 from *P. stipitis* show little or no preference for the aldouronates generated by Xyn11 or Xyn11 and Xyn30 combinations compared to aldouronates generated by Xyn10. Both of these fungal enzymes are secreted and catalyze release of most of the MeG from polymeric $MeGX_n$ with or without the assistance of secreted endoxylanases (Chong et al. 2011;

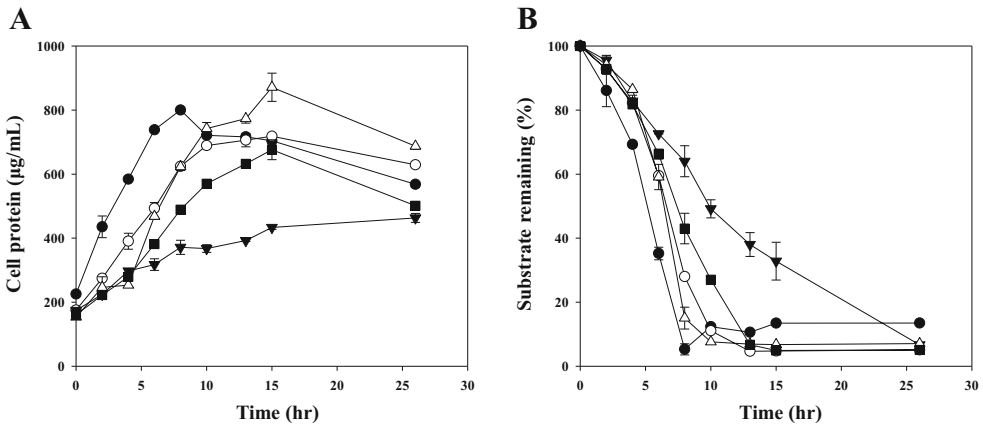

Fig. 5 Growth and aldouronate utilization by Pjdr2. $MeGX_n$ was prepared from sweetgum and served as substrate for the production of aldouronates. XUX and XUXX were prepared from *B. subtilis* lines, UXX from Pjdr2 $Xyn10A_1$ digestion, and U from dilute acid hydrolysates of $MeGX_n$. Cultures containing 0.1 % concentrations of MeGXn (*filled circles*), UXX (*open circles*), XUX (*open triangles*), XUXX (*filled inverted triangles*), and U (*filled squares*) were incubated and analyzed as described in the "Materials and methods" section. **a** Cell protein and **b** carbohydrate utilization

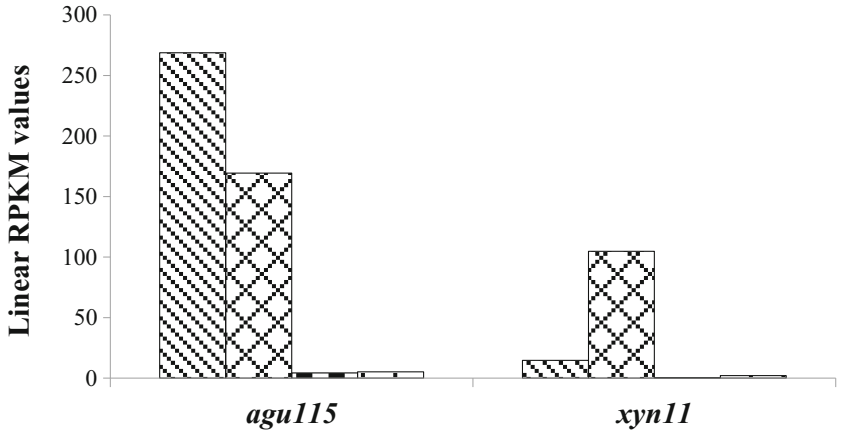

Fig. 6 GH11/GH115 system gene expression in Pjdr2. RPKM (*r*eads *p*er *k*ilobase per *m*illion reads sequenced) values from transcriptomic studies (Sawhney et al. 2015, 2016) following Pjdr2 growth on 0.5 % yeast extract with 0.5 % of either sweetgum $MeGX_n$ (SG ▭), sorghum $MeGAX_n$ (SO ▭), or glucose (G ▭). Cultures with 0.5 % yeast extract without carbohydrate (YE ▭) served as controls for comparison. ANOVA analysis was performed over the entire RNA-seq transcriptome data set, and significant values are judged as having *p* values less then 0.01

Ryabova et al. 2009). Agu115 from *B. ovatus* has also been characterized and shows a preference for XUXX (Rogowski et al. 2014). These differences support different roles in which the secreted fungal GH115 α-glucuronidases may remove MeG substitutions to increase susceptibility to secreted GH10 and GH11 endoxylanases compared to the intracellular bacterial GH115 α-glucuronidases which act on the products of extracellular xylanases after transport into the cells.

Of the three Pjdr2 GH115 genes described above, only Pjdr2_5977 showed upregulation in cultures containing $MeGX_n$ or $MeGAX_n$ (Sawhney et al. 2015), indicating that Pjdr2 Agu115A is the only GH115 utilized by Pjdr2 for xylan processing. The activity of Agu115A from Pjdr2 with XUXX and XUX supports its role in the processing of the aldouronate products generated by the Xyn11 xylanase secreted by Pjdr2. This distinguishes a functional role for this enzyme from the Pjdr2 Agu67 α-glucuronidase which is specific for UXX (Nong et al. 2009). The basis for the Agu67 specificity for UXX, the common product of GH10 xylanases, has been well established in different organisms (Biely et al. 2000; Nagy et al. 2003; Golan et al. 2004).

The structural properties of Pjdr2 Agu115 inferred through homology modeling and its similarity to *B. ovatus* Agu115A are consistent with a functional role for the utilization of the products generated by a Xyn11 enzyme. The signal sequence in *xyn11* and the absence of a signal sequence in *agu115A* predicts that XUXX as well as XUX generated extracellularly are transported into the cell and processed by Agu115A intracellularly to release X_4 and X_3 for catabolism. Support for this role is found in the ability of Pjdr2 to utilize XUXX and XUX for growth (Fig. 5) and by the coordinate expression induction of both these genes in cultures with $MeGX_n$ or $MeGAX_n$ as substrate (Sawhney et al. 2015). The lack of expression of these genes with glucose as substrate (Fig. 6), as well as the identification of catabolite repression (*cre*) sequences within these genes (Table 2), supports coordinate regulation via catabolite repression. As in the case of the genes encoding the GH10/GH67 system in Pjdr2 (Chow et al. 2007), the genes encoding the GH11/GH115 system are likely subjected to glucose repression by the carbon catabolite repression (CCR) system common to the *Firmicutes* (Moreno et al. 2001; Singh et al. 2008). It is surprising that the intracellular Pjdr2 Agu115A is similarly active as the Agu115 enzymes secreted by the fungi, *S. commune* and *P. stipitis*, with respect to their abilities to efficiently catalyze release of MeG from polymeric $MeGX_n$. However, the greater activity of Pjdr2

Table 2 Candidate *cre* sequences upstream of genes

Candidate sequence and distance from translation start site	Similarity to canonical sequence[a]	Gene
5′-TGWAANCGNTNWCA[b]	14	
5′-TGAAAATTAAA#CA*—85 nt—ATG–	10/14 bases	*agu115*
5′-TGTAAA##ATTA#A*—159 nt—ATG–	11/14 bases	*xyn11*

Asterisk indicates candidate *cre* sequence identified from upstream region of these genes; number symbol indicates gap

[a] Number of matching residues/total number of residues in the sequence reflecting similarity to *cre* canonical sequence

[b] The canonical sequence (Cho and Choi 1999); W = A,T and N = A,C,G,T

Agu115 with XUXX and XUX suggests that its role is to complement the Pjdr2 Agu67 enzyme for processing aldouronates imported into the cell.

Options available to Pjdr2 for processing both methylglucuronoxylans and methylglucuronoarabinoxylans are presented in Fig. 7. Pjdr2 contains a gene (locus tag 4367) selectively up-regulated following growth on $MeGAX_n$ compared to $MeGX_n$ that encodes a GH43 glycoside hydrolase (Sawhney et al. 2015). This is an ortholog of the *xynD* gene in *B. subtilis* 168 that encodes an arabinoxylan arabinofuranohydrolase (Axh43) which hydrolyzes arabinofuranosyl residues linked to the 3′ hydroxyl groups of xylose in the xylan chain, converting $MeGAX_n$ to $MeGX_n$ for digestion by endoxylanses (Rhee et al. 2016). The GH10/GH67 system is presumed to utilize the ABC transporter complex containing the UgpB, LplB, and UgpE proteins encoded by genes within a cluster of genes encoding the Agu67A α-glucuronidase, $Xyn10A_2$ endoxylanase, and a putative GH43 β-xylosidase $Xyn43B_1$. The co-regulation of expression of transporter genes along with genes encoding transcriptional AraC and histidine kinase regulatory proteins supports their collective role as a xylan utilization regulon (Chow et al. 2007; Nong et al. 2009). From physiological studies, it is apparent that the GH10/GH67 system allows the rapid and nearly complete utilization of polymeric substrates. Extracellular depolymerization catalyzed by a cell-associated xylanase with carbohydrate-binding domains followed by assimilation of products allows the capture and metabolism of xylose in both aldouronates and oligoxylosides generated during extracellular depolymerization. Based upon transcriptome analysis with $MeGX_n$ and $MeGAX_n$ as substrates, the assimilation of aldouronates generated by Pjdr2 Xyn11 may utilize the same transporters used to assimilate the aldouronates generated by Pjdr2 $Xyn10A_1$ (Sawhney et al. 2015). It is interesting to note than the rate of utilization of UXX generated by $Xyn10A_1$ and XUX generated by Xyn11 is similar and significantly greater that the rate of utilization of XUXX (Fig. 5). This may reflect the use of a common transporter that discriminates on the basis of size of transported aldouronate. The xylan-utilization regulon in Pjdr2 that includes genes encoding Agu67 and the cell-associated Pjdr2 $Xyn10A_1$ also includes structural genes encoding an intracellular $Xyn10A_2$ which, along with a GH43 β-xylosidase ($Xyn43B_1$), may contribute to the processing of X_3 and X_2 following the release of MeG from UXX (Nong et al. 2009). Importation of some of the XUXX may be followed by removal of the nonreducing terminal xylose catalyzed by $Xyn43B_1$ to allow removal of MeG with Agu67 serving as an alternative to removal of MeGA by Agu115A (Fig. 7). The XUX generated by Pjdr2 Xyn11 would presumably be totally dependent on Agu115A for subsequent metabolism. Further definitions of these processes through selective gene deletion are needed.

A recombinant form of the GH115 secreted by *S. commune* has been shown to enhance the bioprocessing of softwood derived from Norway spruce $MeGAX_n$ and significantly increase the release of fermentable sugars above those released by endoxylanases and arabinofuranosidases (McKee et al. 2016). The Pjdr2 Agu115A may be produced in a quantity for addition to enzyme mixtures to enhance the digestion of lignocellulosic resources by defined mixtures of xylanolytic enzymes. In addition to its potential role in processing methylglucuronoxylans with Xyn11, the Pjdr2 Agu115A allows the processing of XUX derived from the combined action of GH11 and GH30 xylanases. *B. subtilis* 168 secretes GH11 and GH30 endoxylanases that synergistically process methyglucuronoxylans to release X_2 and X_3 for metabolism. All of the MeG in methylglucuronoxylans and methylglucuronoarabinoxylans, which may represent on average 1 in 6–12 xyloses, accumulates as XUX which is not

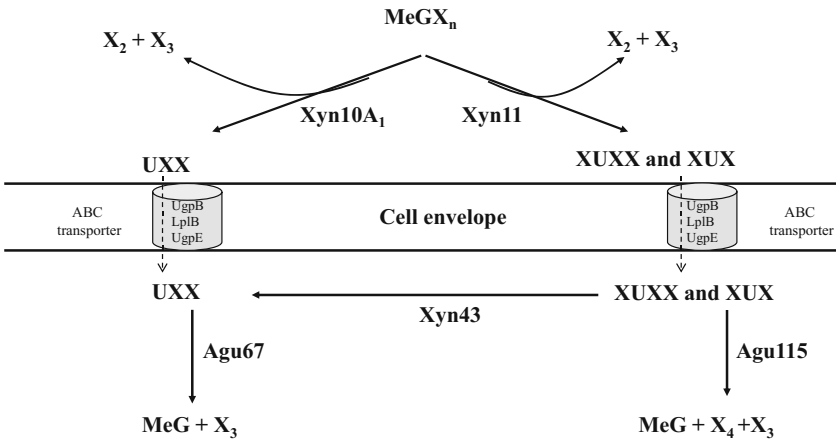

Fig. 7 Scheme for bioprocessing methylglucuronoxylan ($MeGX_n$) by GH10/GH67 and GH11/GH115 systems in *Paenibacillus* sp. JDR-2. Endoxylanases, $Xyn10A_1$ (Pjdr2_0221) and Xyn11 (Pjdr2_4664); α-glucuronidases, Agu67 (Pjdr2_1323) and Agu115A (Pjdr2_5977); possible ABC transporters for aldouronate assimilation, UgpB, LplB, and UgpE (Pjdr2_1320, 1321, 1322); U, methylglucuronosyl residue linked to xylose residue; *X* xylose

metabolized in *B. subtilis* (Rhee et al. 2014). Based upon genome sequences, the GH11/GH30 system for processing xylans is common to many *Bacillus* and *Paenibacillus* spp., providing a resource to other bacteria that encode intracellular GH115 α-glucuronidases. The Pjdr2 Agu115A may then be considered as a candidate for engineering fermentative *Bacillus* and *Paenibacillus* spp. secreting GH30 and GH11 xylanases for developing bacterial biocatalysts to efficiently produce targeted products from lignocellulosic resources.

Acknowledgments This research was supported by Biomass Research and Development Initiative Competitive Grant No. 2011-10006-30358 from the USDA National Institute of Food and Agriculture and by Florida Energy Systems Consortium, State University System of FL, Project No. 00077818.

Compliance with ethical standards

Ethical approval Studies reported in this manuscript did not involve experiments with human or animal subjects.

Conflict of interest The authors declare that they have no conflict of interest.

References

Aalbers F, Turkenburg JP, Davies GJ, Dijkhuizen L, Lammerts van Bueren A (2015) Structural and functional characterization of a novel family GH115 4-*O*-methyl-α-glucuronidase with specificity for decorated arabinogalactans. J Mol Biol 427:3935–3946. doi:10.1016/j.jmb.2015.07.006

Biely P, de Vries RP, Vrsanska M, Visser J (2000) Inverting character of α-glucuriondase A from *Aspergillus tubingens*. Biochim Biophys Acta 1474:360–364

Chen VB, Arendall WB, Headd JJ, Keedy DA, Immormino RM, Kapral GJ, Murray LW, Richardson JS, Richardson DC (2010) MolProbity: all-atom structure validation for macromolecular crystallography. Acta Crystallogr Section D 66:12–21

Cho SG, Choi YJ (1999) Catabolite repression of the xylanase gene (*xynA*) expression in *Bacillus stearothermophilus* no. 236 and *B. subtilis*. Biosci Biotechnol Biochem 63:2053–2058

Chong SL, Battaglia E, Coutinho PM, Henrissat B, Tenkanen M, de Vries RP (2011) The α-glucuronidase Agu1 from *Schizophyllum commune* is a member of a novel glycoside hydrolase family (GH115). Appl Microbiol Biotechnol 90:1323–1332

Chow V, Nong G, Preston JF (2007) Structure, function, and regulation of the aldouronate utilization gene cluster from *Paenibacillus sp*. strain JDR-2. J Bacteriol 189:8863–8870

Chow V, Nong G, St. John JF, Rice JD, Dickstein E, Chertkov O, Bruce D, Detter C, Brettin T, Han J, Woyke T, Pitluck S, Nolan M, Pati A, Martin J, Copeland A, Land ML, Goodwin L, Jones JB, Ingram LO, Shanmugam KT, Preston JF (2012) Complete genome sequence of *Paenibacillus* sp. strain JDR-2. Stand Genomic Sci 6:1–10

Chow V, Sik Kim Y, Rhee M, Sawhney N, St John F, Nong G, Rice JD, Preston JF (2016) Definition of a 1, 3-1, 4-β-glucan-utilization regulon in *Paenibacillus* sp. JDR-2. Appl Environ Microbiol 82: 1789–1798

Chundawat SP, Beckham GT, Himmel ME, Dale BE (2011) Deconstruction of lignocellulosic biomass to fuels and chemicals. Annu Rev Chem Biomol Eng 2:121–145

Dodd D, Cann IKO (2009) Enzymatic deconstruction of xylan for biofuel production. Glob Change Biol Bioenergy 1:2–17

Fujimoto Z, Ichinose H, Biely P, Kaneko S (2011) Crystallization and preliminary crystallographic analysis of the glycoside hydrolase family 115 α-glucuronidase from *Streptomyces pristinaespiralis*. Acta Crystallogr Sect F Struct Biol Cryst Commun 67(Pt 1):68–71

Golan G, Shallom D, Teplitsky A, Zaide G, Shulami S, Baasov T, Stojanoff V, Thompson A, Shoham Y, Shoham G (2004) Crystal structures of *Geobacillus stearothermophilus* α-glucuronidase complexed with its substrate and products. J Biol Chem 279:3014–3024

Han Y, Agarwal V, Dodd D, Kim J, Bae B, Mackie RI, Nair SK, Cann IKO (2012) Biochemical and structural insights into xylan utilization by the thermophilic bacterium *Caldanaerobius polysaccharolyticus*. J. Biol Chem 287:34946–34960

Hurlbert JC, Preston JF (2001) Functional characterization of a novel xylanase from a corn strain of *Erwinia chrysanthemi*. J Bacteriol 183:2093–2100

Kelley LA, Mezulis S, Yates CM, Wass MN, Sternberg MJE (2015) The Phyre2 web portal for protein modeling, prediction and analysis. Nat Protoc 10:848–858

Kolenová K, Ryabova O, Vrsanská M, Biely P (2010) Inverting character of family GH115 α-glucuronidases. FEBS Lett 584:4063–4068

Laemmli UK (1970) Cleavage of the structural proteins during the assembly of the head of bacteriophage T4. Nature 227:680–685

Lynd LR, Wyman CE, Gerngross TU (1999) Biocommodity engineering. Biotechnol Prog 15:777–793

McKee LS, Sunner H, Anasontzis GE, Toriz G, Gatenholm P, Bulone V, Vilaplana F, Olsson L (2016) A GH115 α-glucuronidase from *Schizophyllum commune* contributes to the synergistic enzymatic deconstruction of softwood glucuronoarabinoxylan. Biotechnol Biofuels 9:2–14

Menon V, Rao M (2012) Trends in bioconversion of lignocellulose: biofuels, platform chemicals & biorefinery concept. Prog Energy Combust Sci 38:522–550

Moreno MS, Schneider BL, Maile RR, Weyler W, Saier MH (2001) Catabolite repression mediated by the CcpA protein in *Bacillus subtilis*: novel modes of regulation revealed by whole-genome analyses. Mol Microbiol 39:1366–1381

Mosier N, Wyman C, Dale B, Elander R, Lee YY, Holtzapple M, Ladisch M (2005) Features of promising technologies for pretreatment of lignocellulosic biomass. Bioresour Technol 96:673–686

Nagy T, Nurizzo D, Davies GD, Biely P, Lakey JH, Bolam DN, Gilbert HJ (2003) The α- glucuronidase, GclA67A, of *Cellvibrio japonicus* utilizes carboxylate and methyl groups of aldobiuronic acid as important substrate recognition determinants. J Biol Chem 278:20286–20292

Nelson N (1944) A photometric adaptation of the Somogyi method for the determination of glucose. J Biol Chem 153:375–380

Nong G, Rice JD, Chow V, Preston JF (2009) Aldouronate utilization in *Paenibacillus* sp. strain JDR-2: physiological and enzymatic evidence for coupling of extracellular depolymerization and intracellular metabolism. Appl Environ Microbiol 75:4410–4418

Olson DG, McBride JE, Shaw AJ, Lynd LR (2012) Recent progress in consolidated bioprocessing. Curr Opin Biotechnol 23:396–405

Pettersen EF, Goddard TD, Huang CC, Couch GS, Greenblatt DM, Meng EC, Ferrin TE (2004) UCSF chimera—a visualization system for exploratory research and analysis. J Comput Chem 25:1605–1612

Preston JF, Hurlbert JC, Rice JD, Ragunathan A, St. John FJ (2003) Microbial strategies for the depolymerization of glucuronoxylan: leads to the biotechnological applications of endoxylanases In: Mansfield SD, Saddler JN (eds) Application of enzymes to lignocellulosics, ACS Symposium Series No. 855. pp 191–210 doi: 10.1021/bk-2003-0855.ch012

Ragauskas AJ, Williams CK, Davison BH, Britovsek G, Cairney J, Eckert CA, Frederick WJ Jr, Hallett JP, Leak DJ, Liotta CL, Mielenz JR, Murphy R, Templer R, Tschaplinski T (2006) The path forward for biofuels and biomaterials. Science 311:484–489

Rhee MS, Wei L, Sawhney N, Rice JD, St. John FJ, Hurbert JC, Preston JF (2014) Engineering the xylan utilization system in *Bacillus subtilis* for production of acidic xylooligosaccharides. Appl Environ Microbiol 80:917–927

Rhee MS, Wei L, Sawhney N, Kim YS, Rice JD, Preston JF (2016) Metabolic potential of *Bacillus subtilis* 168 for the direct conversion of xylans to fermentation products. Appl Microbiol Biotechnol 100: 1501–1510

Rogowski A, Baslé A, Farinas CS, Solovyova A, Mortimer JC, Dupree P, Gilbert HJ, Bolam DN (2014) Evidence that GH115 α-glucuronidase activity, which is required to degrade plant biomass, is dependent on conformational flexibility. J Biol Chem 289:53–64

Ryabova O, Vrsanská M, Kaneko S, van Zyl WH, Biely P (2009) A novel family of hemicellulolytic α-glucuronidase. FEBS Lett 583:1457–1462. doi:10.1016/j.febslet.2009.03.057

Saha BC (2003) Hemicellulose bioconversion. J Ind Microbiol Biotechnol 30:279–291

Sawhney N, Preston JF (2014) GH51 arabinofuranosidase and its role in the methylglucuronoarabinoxylan utilization system in *Paenibacillus* sp. JDR-2. Appl Environ Microbiol 80:6114–6125

Sawhney N, Crooks C, St. John FJ, Preston JF (2015) Transcriptomic analysis of xylan utilization systems in *Paenibacillus* sp. JDR-2. Appl Environ Microbiol 81:1490–1501. doi:10.1128/AEM.03523-14

Sawhney N, Crooks C, Chow V, Preston JF, St. John FJ (2016) Genomic and transcriptomic analysis of carbohydrate utilization in *Paenibacillus* sp. JDR-2: systems for bioprocessing plant polysaccharides. BMC Genomics 17:131–147

Shaw AJ, Podkaminer KK, Desai SG, Bardsley JS, Rogers SR, Thorne PG, Hogsett DA, Lynd LR (2008) Metabolic engineering of a thermophilic bacterium to produce ethanol at high yield. Proc Natl Acad Sci U S A 105:13769–13774

Shulami S, Gat O, Sonenshein AL, Shoham Y (1999) The glucuronic acid utilization gene cluster from *Bacillus stearothermophilus* T-6. J Bacteriol 181:3695–3704

Sievers F, Wilm A, Dineen D, Gibson TJ, Karplus K, Li W, Lopez R, McWilliam H, Remmert M, Söding J, Thompson JD, Higgins DG (2011) Fast, scalable generation of high-quality protein multiple sequence alignments using Clustal Omega. Mol Syst Biol 7:539

Singh KD, Schmalisch MH, Stülke J, Görke B (2008) Carbon catabolite repression in *Bacillus subtilis*: quantitative analysis of repression exerted by different carbon sources. J Bacteriol 190:7275–7284

St. John FJ, Rice JD, Preston JF (2006a) *Paenibacillus* sp. JDR-2 and XynA1: a novel system for methylglucuronoxylan utilization. Appl Environ Microbiol 72:1496–1506. doi:10.1128/AEM.72.2.1496-1506.2006

St. John FJ, Rice JD, Preston JF (2006b) Characterization of XynC from *Bacillus subtilis* subsp. *subtilis* strain 168 and analysis of its role in depolymerization of glucuronoxylan. J Bacteriol 188:8617–8626

Su Y, Rhee MS, Ingram LO, Shanmugam KT (2011) Physiological and fermentation properties of *Bacillus coagulans* and a mutant lacking fermentative lactate dehydrogenase activity. J Ind Microbiol Biotechnol 38:441–450

Talluri S, Raj SM, Christopher LP (2013) Consolidated bioprocessing of untreated switchgrass to hydrogen by the extreme thermophile *Caldicellulosiruptor saccharolyticus* DSM 8903. Bioresour Technol 139:272–279

Tenkanen M, Siika-aho M (2000) An α-glucuronidase of *Schizophyllum commune* acting on polymeric xylan. J Biotechnol 78:149–161

Waterhouse AM, Procter JB, Martin DMA, Clamp M, Barton GJ (2009) Jalview version 2—a multiple sequence alignment editor and analysis workbench. Bioinformatics 25:1189–1191

Weber C, Farwick A, Benisch F, Brat D, Dietz H, Subtil T, Boles E (2010) Trends and challenges in the microbial production of lignocellulosic bioalcohol fuels. Appl Microbiol Biotechnol 87:1303–1315

Yang J, Yan R, Roy A, Xu D, Poisson J, Zhang Y (2015) The I-TASSER Suite: protein structure and function prediction. Nat Methods 12:7–8

Yoon SA, Moon TS, Iranpour P, Lanza AM, Prather KJ (2009) Cloning and characterization of uronate dehydrogenase from two pseudomonads and *Agrobacterium tumefasciens* strain C58. J Bacteriol 191: 1565–1573

Zucker M, Hankin L (1970) Regulation of pectate lyase synthesis in *Pseudomonas fluorescens* and *Erwinia carotovora*. J Bacteriol 104:13–18